International Journal of Power and Energy Systems, Vol. 42, No. 10, 2022
An Open Access Paper

MULTI-OBJECTIVE CHAOTIC MAYFLY OPTIMIZATION FOR SOLAR-WIND-HYDROTHERMAL SCHEDULING BASED ON ATC PROBLEM

Kingsuk Majumdar,* Provas K. Roy,** and Subrata Banerjee***

Abstract

The electrical power generation from conventional thermal power plants needs to be interconnected with natural resources like solar, wind, hydro units with all-day planning and operation strategies to save mother nature and meet the current electricity demand. The complexity and size of the power network are increasing rapidly day by day. The enhanced power transfer from one section to another section in the existing grid system is the subject of available transfer capability (ATC), which is the modern power system's critical factor. In this paper, the minimization of power generation cost of the thermal power units is achieved by incorporating renewable sources, says hydro, winds, and solar plants for 24 h scheduled, and ATC calculation is the prime objective. In recent literature, the Mayfly algorithm (MA) optimization approach, which combines the advantages of evolutionary algorithms and swarms intelligence to attend better results, is successfully implemented. In this article, optimum power flow-based ATC is enforced under various conditions with hydro-thermal-solar-wind scheduling concept on the IEEE 9 test bus system to check the performance of the proposed chaotic MA. The chaotic MA is a hybridized format of the MA and chaotic map (CHMA) method. It is noted from the simulation study that the suggested CHMA approach has a dominant nature over other well-established optimization algorithms. In case of single objective function, the value of the cost function is improved by 14% and that of for multi-objective, it is improved by more than 20% and ATC value is enhanced by near about 55% and more.

Key Words

Available transfer capability (ATC), chaotic Mayfly algorithm (CHMA), hydro-thermal-solar-wind scheduling (HTSW), Mayfly algorithm (MA), optimum power flow (OPF), and particle swarm optimization (PSO)

* Department of Electrical Engineering, Dr. B C Roy Engineering College, Durgapur, Durgapur, West Bengal, 713206, India; e-mail: kingsuk.majumdar5@gmail.com
** Kalyani Government Engineering College, Kalyani, Department of Electrical Engineering, West Bengal, India; e-mail: roy_provas@yahoo.com
*** Department of Electrical Engineering, National Institute of Technology, Durgapur, Durgapur, West Bengal, 713209, India; e-mail: bansub2004@yahoo.com
Recommended by Prof. Ikhlaq Hussain
(DOI: 10.2316/J.2022.203-0382)

1. Introduction

In the present era, to save mother nature and reduce the thermal power plant's generation cost, natural resources are involved. In this paper, solar, hydro, and wind power plants are incorporated with conventional thermal units to achieve the goal. The authors have also done 24 h load scheduling and proper coordination of all the said natural resources with thermal units to match the load demand. The North American Electric Reliability Council (NAERC) defines available transfer capability (ATC) as the amount of extra transportable power through the existing transmission system without violating power system constraints. As per the guideline of Federal Energy Regulatory Commission (FERC), the basic ATC data must be available on an hourly basis in an open−access market. The distribution generations (DGs) add up to the complexity of the modern power system framework. It is to enhance the capacity of transferring electrical power in the existing network for future transaction to deal with contingencies and uncertainties of the power system [1]. In the present era, with the rising economy, power transfers have been enhancing at a much higher rate than transmission capacity, which abbreviated reliability and system security. ATC assessment is the window to provide adequate knowledge in advance on these types of power transactions through the existing electrical power network without violating the power system constraints [1]–[3].

Estimating any parameter in real-time adds an extra huddle to its evaluation process like ATC calculation. This real-time ATC evaluation gives ample benefits in financial and engineering aspects as follows:

1. If the ATC knowledge is known in advance, more operating windows will be opened for the operator to run the power system in ten times or more power transaction conditions.

2. The development and implementation of natural resources like wind-solar-hydro and the smart grid inject more uncertainties, making real-time ATC determination a hard nut to crack [2].
3. The on-line study can be boiled down to those cases relevant to actual operating circumstances.

In early growths of ATC estimation depends on the network's power flow; hence, their computational speed is high. However, the modern power system consisting of a grid and large-scale DGs make electrical power flow equations complex and non-linear in nature. Therefore, to estimate the value of ATC by most of the linearized methods cannot be implemented easily, as it involves voltage stability, thermal limit, reactive power generation limit, and other power system constraints. In the present era, several computational methods have been investigated for the same as follows:

- in view of optimal power flow (OPF) approach [4];
- as a distributed state estimations process;
- with the concept of distributed control for distribution networks;
- conceding voltage stability monitoring [5];
- with distributed contingency analysis method [6];

Particle swarm optimization (PSO), grey wolf optimizer (GWO), Mayfly Algorithm (MA), and chaotic Mayfly algorithm (CHMA) optimization are incorporated with the OPF concept to achieve accurate estimation of ATC without violating power system constraints parameters. This article aims to furnish the estimated ATC by subdividing it into some zone of areas and, more preciously say, using tie-line. Therefore, the ATC estimation can be formulated as a distributed multi-area OPF problem considering both inequality and equality criteria. Due to the enormous development of computational power in modern days, computation time and memory complexity are no longer a great deal. By proper coordinated and distributed mechanism, the ATC of the entire power grid can be obtained in real time. In brief, the prime objectives of this paper can be enlisted as follows:

1. The thermal-hydro-wind-solar scheduling along with of variation of demands for 24 h are taken into consideration during the problem formulation in this article [7].
2. To reduce the cost of generation and to save the environment, thermal power plants are coordinated with hydro-wind-solar units.
3. Generally, ATC is calculated without considering the generation cost. In this article, generation cost is also taken into consideration, which makes the said problem multi-objective optimization [8].
4. The multi-objective ATC problem is formulated using OPF concept along with multi-objective MA algorithms.

The rest of this paper is organised as below: In Section 2, the mathematical modelling is fabricated, as mentioned earlier, associated with the thermal unit and other natural energy sources like wind, solar, and hydro. In the following section, proposed single and multi-objective MA optimization is described vividly. Afterwards, the application of the mechanism as mentioned earlier has been studied for standard IEEE 9-bus system under different test cases in Section 4. Finally, the future scope and conclusion have been discoursed in Section 5.

2. Mathematical Modelling of the System

In this mathematical modelling section, the active power generation with 24 h scheduling and ATC estimation has been done step by step. This scheduling has machinated in coordination among thermal, wind, solar, and hydro plants.

2.1 Wind Power Generation and Its Generation Cost

The generation of wind energy from wind is uncertain due to the variation in wind speed. The wind speed can be predicted using probability density function (1) as follows:

$$pdw(S_{1h}, S_{1f}, vl) = \exp\left(-\left(\frac{vl1}{S_{1f}}\right)^{S_{1h}}\right) * \frac{S_{1h}}{S_{1f}}\left(\frac{vl1}{S_{1f}}\right)^{S_{1h}-1} \tag{1}$$

The cumulative density function (CDF) termed as *pdw* for the wind speed can be expressed as below (2):

$$cdw(S_{1h}, S_{1f}, vl1) = 1 - \exp\left[-\left(\frac{vl1}{S_{1f}}\right)^{S_{1h}}\right] \tag{2}$$

The relation between wind velocity and wind power is represented by a linear model as the generation of wind power depends on the velocity of the wind (3)

$$wnd = \left\{\begin{array}{l} wnd_{1R};\ vl_{1R} \leq vl \leq vl_{1out} \\ 0;\ vl < vl_{1in} \text{ or } vl \geq vl_{1out} \\ \dfrac{wnd\,(vl - vl_{1in})}{vl_{1R} - vl_{1in}};\ vl_{1in} \leq vl \leq vl_{1out} \end{array}\right\} \tag{3}$$

The authors have calculated the probability of wind power as *wnd* and zero wind condition by using (3) as follows:

$$\begin{aligned} &P_{wnd}\,(wnd = 0) = cdw\,(vl_{1in}) - (cdw\,(vl_{1out}) - 1) \\ &= 1 + \exp\left(-\left(\frac{vl_{1out}}{S_{1f}}\right)^{S_{1h}}\right) - \exp\left(-\left(\frac{v1l_{in}}{S_{1f}}\right)^{S_{1h}}\right) \end{aligned} \tag{4}$$

where cfw of the random variable (wnd) by considering (4) can be written as follows:

$$f_{wnd}(1wnd) = \begin{cases} 1; wnd > wnd_{1R} \\ 0; wnd < 0 \\ \begin{cases} \dfrac{Vl_{1in}S_h H_{wnd}}{Wnd_R S_f}\left(\dfrac{(wnd_{1R}+H_{1wnd})Vl_{1in}}{wnd_{1R}S_{1f}}\right) \\ \times \exp\left(-\dfrac{(wnd_{1R}+H_{1wnd})Vl_{1in}}{wnd_{1R}S_{1f}}\right); \\ 0 < wnd \leq wnd_{1R} \end{cases} \end{cases} \tag{5}$$

where

$$H_{1wnd} = -1 + \left(\frac{vl_{1R}}{vl_{1in}}\right) \tag{6}$$

Wind power production is not steady due to wind speed; hence, wind power is sometimes less than the demand (overestimated scenario) or more than load demand (underestimated scenario) [9]. Two additional cost terms are involved: overestimation and underestimation cost, respectively, and are joined to both cases of wind power generation. The underestimation and overestimation cost formulas can be jotted as follows:

$$\begin{aligned} E_{1wnd,1Z,1T} = {} & C_{1wnd,1Z}(wnd_{1R,1Z} - wnd_{1Z,1T}) \left\{ \exp\left(-\left(\frac{Vl_{1in,1Z}}{S_{1f,1Z}}\right)^{S_{1h,1Z}}\right) - \exp\left(-\left(\frac{Vl_{1out,Z}1}{S_{1f,1Z}}\right)^{S_{1h,1Z}}\right)\right\} \\ & + \left\{ \exp\left(-\left(\frac{Vl_{1in,1Z}}{S_{1f,1Z}}\right)^{S_{1h,1Z}}\right) - \exp\left(-\left(\frac{Vl_{1in,1Z}}{S_{1f,1Z}}\right)^{S_{1h,1Z}}\right)\right\} \left\{ wnd_{1Z,1T} + \frac{wnd_{1R,1Z}Vl_{1in,1Z}}{v_{1in,1Z} - v_{1out,1Z}} \right\} \\ & + \left\{ \Gamma\left\{ \left(\frac{1}{S_{1h,1Z}}\left(\frac{Vl_{1in}}{S_{1f,1Z}}\right)^{S_{1h,1Z}}\right) + 1 \right\} + \Gamma\left\{ \left(\frac{1}{S_{1h,1Z}}\left(\frac{Vl_{1R,1Z}}{S_{1f,1Z}}\right)^{S_{1h,1Z}}\right) + 1 \right\} \right\} \frac{wnd_{1R,1Z}S_{1f,1Z}}{Vl_{1R,1Z} - Vl_{1in,1Z}} \end{aligned} \tag{7}$$

To match the demand, it is required to purchase the power from the wind farm operator, which is called direct cost of wind power, and it can be formulated as follows: (8)

$$E_{dr.1Z.1T} = wnd_{1Z.1T} \times g_{1Z} \tag{8}$$

Therefore, the wind power generation considering under and overestimation and direct cost of wind generation for each interval are as follows (9):

$$\begin{aligned} E_{wnd\_tot} = \sum_{1Z=1}^{N_{1wnd}} \sum_{t=1}^{1T_{hor}} \Big(& E_{dr.1Z.1t} \\ & + E_{UN.1Z.1t} + E_{1OVR.1Z.1t} \Big) \end{aligned} \tag{9}$$

where N_{1wnd} is the total number of wind generators.

2.2 Solar Power Generation and Its Generation Cost

The power generation from a solar plant depends on the incident solar radiation (SI_s) and the ambient temperature (T_{amb}) [10]. Therefore, the solar power generation can be expressed as follows:

$$SP_{1solar} = PS_{1solar} \times \frac{SI_1 s}{1,000} \times \{\alpha_s(T_{1ref} - T_{1amb}) + 1\} \tag{10}$$

The total solar share (S_{tot}) from installed units are controlled as OFF/ON state of solar panel.

$$S_{1tot} = \sum_{solar=1}^{ns} SP_{solar,1t} \times U_{solar,1t} \tag{11}$$

The solar share, *i.e.,* S_{1tot} maximum limit is limited to x_{solar}% of the total demand power at any subinterval of $1t$ of total interval T can be formulated mathematically as follows:

$$S_{1tot} \leq x_{solar} \times PD_t \tag{12}$$

The cost of the solar share is represented as follows:

$$F_{solar} = \sum_{t=1}^{1T} \sum_{solar=1}^{ns} S_{s_{1tot},1t} \times PUcost_{solar} \tag{13}$$

To grab the optimum benefit from the installed solar capacity, a penalty factor is implemented. Therefore, the cost of mismatch between installed power capacity and generated solar power is represented as follows:

$$F_{solar} = Pn_s \times \sum_{t=1}^{T} \sum_{solar=1}^{ns} (SP_{solar,t} - S_{solar,t}) \tag{14}$$

2.3 Hydro Power Generation and Its Generation Cost

The running cost of a hydro power generation unit is negligible as it is very low. Hence, hydro power generation unit can be combined with thermal power plant to reduce its fuel and emission cost. The hydro power generation $PHY_{i,t}$ is related to discharge rate of water and storage volume and can be formulated as follows:

$$\begin{aligned} PHY_{i,1t} = {} & CHi_{6,1t} + CHi_{5,1t}disq_{i,1t} + CHi_{4,1t}Vol_{i,1t} \\ & + CHi_{3,1t}disq_{i,1t}Vol_{i,1t} + CHi_{2,1t}Vol_{i,1t}^2 \\ & + CHi_{1,1t}disq_{i,1t}^2 \end{aligned} \tag{15}$$

where $CHi_{1,1t}$, $CHi_{2,1t}$, $CHi_{3,1t}$, $CHi_{4,1t}$, $CHi_{5,1t}$, and $CHi_{6,1t}$ are coefficient of the hydro generation unit; $Vol_{i,t}$ and $disq_{i,1t}$ are volume of water of i^{th} units and discharge rate of i^{th} unit, respectively .

2.4 Thermal Power Generation and Its Generation Cost

Thermal power generator is generally represented with valve point effect along with quadratic function [11] as shown below:

$$\begin{aligned} F_{Th\_tot} = \sum_{t=1}^{T} \sum_{i=1}^{N_{genTH}} & (\alpha_i P_{th_i}^2 + \beta_i P_{th_i} + \gamma_i \\ & + \mid e_{1_i} \sin(e_{2_i}(-P_{thmin_i} + P_{th_i})) \mid) \end{aligned} \tag{16}$$

where α_i, β_i, γ_i are the fuel coefficients, e_{1_i}, e_{2_i} are the valve point loading effect constants, and P_{thmin_i} is the minimum active power generation of the i^{th} thermal unit. The total number of thermal generator is N_{genTH}.

Therefore, the active power generation cost for thermal unit along with solar, wind, and hydro unit can be formulated as below:

$$\begin{aligned} F_{gen\_tot} &= F_{solar} + E_{wnd\_tot} + F_{Th\_tot} \\ &+ \gamma_w \sum_{t}^{H} \sum_{i=1}^{N_{genHY}} PHY_{i,t} \end{aligned} \quad (17)$$

where γ_w is a scalar constant which converts water volume discharge to equivalent generation cost.

2.5 Problem Formulation of ATC Along with HTSW Scheduling

In this article, the OPF concept is employed to face the challenges of ATC. The cost function, *i.e.*, the objective function is originated at possible maximum power flow from a particular zone of generating units in a source area to the load buses in a sink area through some specific transmission or tie-lines without assaulting the power system operation constraints and limits. The thermal limit of a line is taken as an upper limit of the particular line's power transaction. The cost function for ATC based on OPF is formulated mathematically. Generally, for ATC problem, active power generation cost is not considered, but here both ATC and power generation cost are considered. In this paper, mainly two different cases are considered as follows:

- CASE A: Minimization of active power generation cost alone (using HTSW scheduling)
- CASE B: Maximization of ATC along with minimization of active power generation cost with renewable energy sources (multi-objective).

Therefore, the cost function can be formulated as below:

$$F_{Tot} = \psi_{TL} F_{TL} + \psi_{TLA} F_{TLA} + \psi_V F_{Vmis} + \psi_{gen} F_{gen\_tot} \quad (18)$$

where ψ_{TL}, ψ_V, ψ_{TLA} , and ψ_{gen} are different positive scalar values for the objective function. Given suitable weight, on these scalar factors, single or/and multi-objection cost function can be achieved. For enhancement of ATC, power flow should be raised through some particular lines and can be shown as

$$F_{TLA} = \left| \left(\frac{1}{S_{TLi} - S_{TLBi}} \right) \right| \quad (19)$$

where S_{TLi} and S_{TLBi} are power flow through the ith line and base power flow through the line, respectively. To confine overloading of transmission line, a mathematical factor is introduced in the cost function as follows:

$$F_{TL} = \sum_{i=1}^{NTL} \left(S_{TL\max_i} - S_{TL_i}\right)^2 \quad if S_{TL\max_i} < S_{TL_i} \quad (20)$$

Table 1
Value of Different Cost Scalar Factors at Different Cases

Case	ψ_{TL}	ψ_V	ψ_{TLA}	ψ_{gen}
Case A	1,000	1,000	0	1
Case B	20	20	10	0.001

The equality constrains of the load flow are as follows:

$$P_{G_i} - P_{D_i} - \sum_{j=1}^{NBUS} V_i Y_{ij} V_j \cos(\theta_{ij} + \delta_j - \delta_i) = 0 \quad (21)$$

$$Q_{G_i} - Q_{D_i} + \sum_{j=1}^{NBUS} V_i Y_{ij} V_j \sin(\theta_{ij} + \delta_j - \delta_i) = 0 \quad (22)$$

The voltage, active power, and reactive power generation constraints are as follows:

$$V_i^{\min} \le V_i \le V_i^{\max}; i = 1, \ldots, NBUS \quad (23)$$

$$P_{Gi}^{\min} \le P_{G_i} \le P_{Gi}^{\max}; i = 1, \ldots, NGEN \quad (24)$$

$$Q_{Gi}^{\min} \le Q_{G_i} \le Q_{Gi}^{\max}; i = 1, \ldots, NGEN \quad (25)$$

where $NBUS, NGEN$ are total number of bus and generator bus, respectively, and $V_i^{\max}, P_{Gi}^{\max}, Q_{Gi}^{\max}$ and $V_i^{\min}, P_{Gi}^{\min}, Q_{Gi}^{\min}$ are maximum and minimum voltages, active and reactive power generation limits, respectively, in the IEEE test system.

The shunt reactor compensations and tap setting transformer of the test system can be represented, respectively, as follows:

$$Q_{SHi}^{\min} \le Q_{SHi} \le Q_{SHi}^{\max}; i = 1, \ldots, NSH \quad (26)$$

$$T_i^{\min} \le T_i \le T_i^{\max}; i = 1, \ldots, NT \quad (27)$$

where NSH, NT are total number shunt reactors and tap-transformers and super subscript min and max are their minimum and maximum values, respectively. In (18), the scalar constants have different value at different case conditions and are tabulated in Table 1.

3. Proposed Algorithms and Their Implementation

In this section, different types of meta-heuristic algorithms including the proposed multi-objective CHMA are discussed to solve the said problems.

3.1 The Proposed Mayfly Algorithm

Mayflies [12] are part of an ancient group of insects called palaeoptera, which are insects that belong to the order ephemeroptera. The proposed MA optimization method is a potent hybrid algorithmic structure that is an upgradation of PSO [13] and considering the critical advantages of PSO, GA [14] and MA [15]. The social behaviour of mayflies, especially their mating process, is the backbone of the proposed algorithm. It is assumed that mayflies are already adults and the fittest mayflies survive after hatching from the egg, irrespective of how long they live.

The position of each mayfly in the search space represents a potential solution to the proposed problem. The algorithm works as follows. Initially, two sets of mayflies are randomly generated, representing the male and female populations, respectively. In the said algorithm, each mayfly is randomly located in the N-dimensional problem search space as a candidate solution, represented as a vector $x_i = (x_{i_1}, x_{i_2}, \ldots, x_{i_N})$ and $y_i = (y_{i_1}, y_{i_2}, \ldots, y_{i_N})$ for male and female mayfly, respectively. The velocity of the same is presented by $v_i = v_{i_1}, v_{i_2}, \ldots, v_{i_N}$. The direct of movement and trajectory of each mayfly is influenced by individual best (P_{ibest}) and global best (g_{best}).

3.1.1 Movement of Male Mayflies

Males are gathering in swarms implies that each male mayfly's position adjusted according to both its own experience and that of its neighbours. The current position ($x_j^{t_0+1}$) and velocity ($v_{ji}^{t_0+1}$) of the j^{th} mayfly are represented, respectively, as follows:

$$x_j^{t_0+1} = v_j i^{t_0+1} + x_j^{t_0} \tag{28}$$

$$v_j i^{t_0+1} = v_j i^{t_0} + A(pbest_{ji} - x_{ji}^{t_0}) + B(gbest_i - x_{ji}^{t_0}) \tag{29}$$

3.1.2 Movement of Female Mayflies

The female mayflies do not gather in a swarm like males; instead, they fly towards males to breed. The velocity and position of the female mayfly can be represented as follows:

$$v_{ji}^{t_0+1} = \left\{ \begin{array}{l} rand(1,-1) * fl + v_{ji}^{t_0}; \text{if } f(y_j) \leq f(x_j) \\ -\, a_2 * exp(-\beta r^2 m_f) * (y_{ji}^{t_0} - x_{ji}^{t_0}) + v_{ji}^{t_0}; \\ \text{if } f(x_j) < f(y_j) \end{array} \right\} \tag{30}$$

where fl is a random walk coefficient used when a female is not attracted by a male, r_{mf} is the Cartesian distance between male and female mayflies, and β is a fixed visibility coefficient. Finally, rand(1, -1) gives random number in between 1 and -1.

3.1.3 Mating of Mayflies

The crossover represents the mating process between two mayflies: two different genders are taken from their population as parents. The way parents are selected the same as males attract the females. Notably, the selection can be either based on their fitness function value or random. In the latter, the best female breeds with the best male, the second-best female with the second-best male like that. Each cross over produces two offspring and mathematically can be expressed as follows:

$$off_1 = (1 - L) * F + L * M \tag{31}$$

$$off_2 = (1 - L) * M + L * F \tag{32}$$

where L is the random value in the specific range, M, L stand for male and female parents, respectively. Finally, off_1 and off_2 are off springs whose initial velocities are set to zero.

3.2 Chaotic Maps

In this section, the authors have described the proposed hybrid MA algorithm that uses the chaotic scale factor concept. The primary factor and condition sensitivity are the main concerns in a chaotic system. The chaos concept has played a crucial role in the initialization process of said MA. Hence, this article gives the hybridization of chaos and MA to achieve better convergence of the problem. In general, the chaotic combinations are non-linear stimulation systems and, hence, responsiveness depends on both system parameter variations and initial expressions [16], [17]. There are a lot of different chaotic maps that have been proposed in different literature. In this article, ten different chaotic maps are taken under consideration, *i.e.*, circle, cubic, logistic, Gaussian/mouse, sinusoidal, sine, singer, tent, piece-wise, and iterative [18]. Those mentioned above, ten chaotic maps are incorporated with MA algorithms during the generation of MA's initial population for the rest of the simulation study. Afterwards, the relevant chaotic map is selected to implement in the IEEE 9-bus system under different cases.

3.3 Implementation of Chaotic MA into Proposed Problem

In this section of the paper, the implementation of proposed hybrid chaotic MA is discussed as follows:

- Step I: Randomly generate the initial population with various chaotic mapping and check for feasibility.
- Step II: Evaluate position and velocity of female and male using (29), (30), and (31)
- Step III: Calculate the pbest and gbest of population
- Step IV: Ranking and evaluation of off springs are done using (32) and (33)
- Step V: Randomly separate female and male off springs
- Step VI: Exchange worst solutions with the best new ones
- Step VII: Update pbest and gbest
- Step VIII: If maximum iteration is not reach go to Step II else next Step
- Step IX: Print all best control variables and show the convergence curve and voltage profile.

The different types of chaotic maps are used in various literature [18], say Circle chaotic map, Cubic chaotic map, Logistic chaotic map, Gaussian/mouse chaotic map, Sine chaotic map, Sinusoidal chaotic map, Singer chaotic map, Piece-wise chaotic map, Tent chaotic map, Iterative chaotic map, are marked as CH1, CH2, CH10, respectively. In the algorithm mentioned above, CH10 (*i.e.*, Iterative chaotic map) chaotic map can be replaced by any other one. But it is observed that CH10 is better than others concerning the said problem. Hence, it is hybridized with basic MA (CHMA10 or simply CHMA).

4. Results and Discussion

In this article, one standard test system say IEEE 9-bus system is taken to examine the effectiveness of the proposed algorithms. The IEEE 9-bus test system data have been

Table 2
Cost Comparison of Various Methods Under Different Strategies of 9-bus System for 24 h

Methods	mini total fitness cost	ave total fitness cost	worst total fitness cost	ATC (24 h)	only gen cost	Thermal Gen cost	Wind cost	Solar Cost	line flow violation	no of trial	simulation time(s)
CASE A: only generation cost optimization											
SCA-ELS [19]	18,268.57	NA	NA	NA	18,268.57	NA	NA	NA	NA	NA	19
PSO	18,700.9047	18,721.5379	1,886.8714	0.0162	18,700.9047	14,132.3654	3,854.3241	714.2152	0	30	33
GWO	16,142.5623	16,149.5622	16,153.8209	0.0191	16,142.5623	12,268.3473	3,228.5125	645.7025	0	30	28
MA	16,056.0662	16,067.6012	16,125.7568	0.0198	16,056.0662	9,001.2100	6,292.3321	762.5241	0	30	39
CHMA	15,900.9198	15,935.2188	15,943.5534	0.0172	15,900.9198	8,953.3046	6,192.9177	754.6975	0	30	63
CASE B: multi-objective											
PSO	311.8312	352.3082	440.6068	0.0345	21,976.2197	14,215.7114	7,124.2542	636.2541	0	30	37
GWO	267.1627	271.5997	277.4751	0.0406	20,857.3255	13,765.8348	6,465.7709	625.7198	0	30	35
MA	210.4622	228.3994	249.2060	0.0534	23,123.2454	12,744.824	9,901.8138	476.6076	0	30	45
CHMA	209.7739	218.3847	223.7901	0.0536	23,127.9505	12,754.0536	9,902.844	471.0529	0	30	89

taken from MATPOWER tool box, and each test case and each optimization are taken for 30 trial run. The initial population are taken as 50 for all individual case. All test cases have been implemented on HP system with Intel Core i3, 1.8 GHz processor, Windows 10 (home) operating system with 8 GB of DDR3 RAM memory and Matlab 2016a. In this article, the 10 different chaotic maps are implemented on 9 bus system for condition CASE A with 30 random trial runs and their comparative study has been done. It is observed that the iterative chaotic map, *i.e.,* CM10 along with MA provides the best results compared to others chaotic maps of hybridization. Therefore, through out the article, iterative chaotic map hybridization with MA is taken into consideration for all the cases of study. All the water discharge is in the tables are to be multiplied with 10^5cu-m.

4.1 9-bus Test System Study and Result

In the 9-bus test system, there are 9 buses, 6 number of generating units, among them two are hydro units, one is wind unit, two are solar unit (consist of 13 panels for each) and one is thermal unit. There are three load buses (*e.g.* buses 5, 7, and 9), and the active and reactive loads are marked as (PD1, PQ1), (PD2, PQ2), and (PD3, PQ3), respectively. Line number 2, *i.e.,* from bus 4 to bus 5 is taken for ATC calculation in this article. The control variables for IEEE 9-bus test system are 2 discharges for 2 hydro units, active power generation of 1 thermal unit, 1 wind and 2 solar generations along with 6 generating bus voltage, 2 tap setting transformer tap position, and 2 shunt compensation VAr. Therefore, total control variables are taken as 16. Two cases are studied one after another. In first case, *i.e.,* CASE A, the authors have focused to minimize generation cost only.

In Table 2, minimization of total cost after 30 random trial run using PSO is found to be 18,700.9047 \$/24 h which is inferior to those obtained using sine cosine algorithm (SCA) of 18,268.5700 \$/24 h [19]. Moreover, GWO gives better result for the same as 16,142.5623 \$/24 h, and the proposed algorithm along with CM10 method produces the best result as 15,900.9198 \$/24 h, and it is also noticeable that in this case total thermal cost is reduced by 14.89%.

It is observed that 13 solar panels in each solar units have two states either ON or OFF, denoted as “1” and “0,” respectively. Finally, the authors have discussed about multi-objective optimization by minimization of overall cost along with ATC maximization, *i.e.,* CASE B. It is observed that again CHMA technique produces best results as 209.7739 \$/24 h among other proposed algorithms considering 30 individual triaz runs and observed that there is a 48.65% cost reduction compared to PSO technique. Furthermore, among the 30 individual trail runs in each study case, minimum (best), average values, and the maximum (worst) of production costs of other methods are summarized in Table 2 and Fig. 1 shows the costs (\$/24 h) of different discussed algorithms for all cases. It is observed

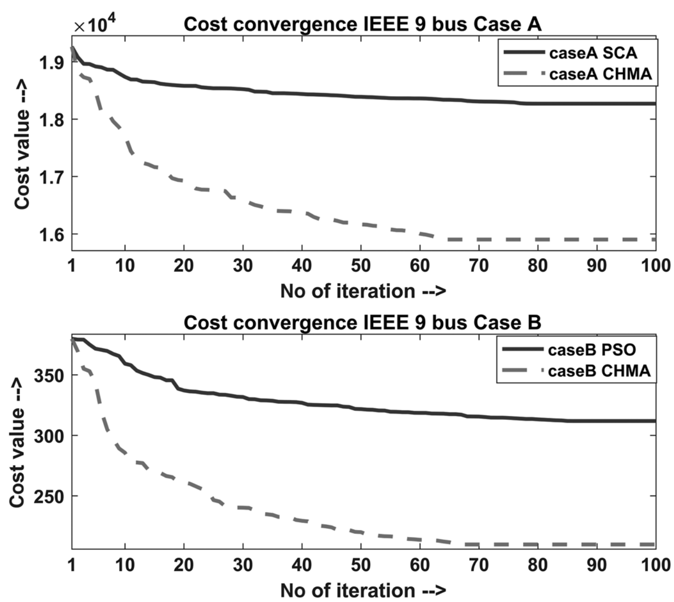

Figure 1. Cost convergence 9-bus test system under various scenario.

from Table 2, in the case of CHMA, the ATC is enhanced by 55.36% compared to PSO. The simulation results reveal the computational efficiency of the proposed CHMA approach.

5. Conclusion

This paper introduces a recent methodology for enhancing ATC and generation of cost optimization incorporating renewable sources, *i.e.*, hydro, solar, and wind [20]. The proposed method, *i.e.,* CHMA method, has been verified by examining its superior convergence characteristics and higher efficiency with other meta-heuristic optimizations. The uncertainties of wind power and load requirement are taken into consideration in this article. The incorporation of solar, wind, and hydro units to the traditional thermal generating units to minimize the overall active power generation cost is another objective of this paper. The results executed by the projected approach are correlated through the results established by the similar heuristic methods, say SCA, PSO, GWO, MA, revealed in the current literature. The efficiency of the proposed method is substantiated by using IEEE 9-bus test system for two different cases. In each case, the proposed method shows that convergence characteristics and computational efficiency of CHMA are superior to that of the other methods. This article handles the problems regarding ATC with hydro-thermal and solar and wind scheduling for 24 h [21], which is the uniqueness of this paper.

References

[1] A.R. Bergen, *Power Systems Analysis* (Pearson Education India, 2009).

[2] G.C. Ejebe, J. Tong, J. Waight, J. Frame, X. Wang, and W. Tinney, Available transfer capability calculations, *IEEE Transactions on Power systems*, *13*(4), 1998, 1521–1527.

[3] H.-D. Chiang and H. Li, *On-Line ATC Evaluation for Large-Scale Power Systems: Framework and Tool* (Springer, 2005).

[4] A.G. Bakirtzis and P.N. Biskas, A decentralized solution to the DC-OPF of interconnected power systems, *IEEE Transactions on Power Systems*, *18*(3), 2003, 1007–1013.

[5] L. Xie, Y. Chen, and H. Liao, Distributed online monitoring of quasi-static voltage collapse in multi-area power systems, *IEEE Transactions on Power Systems*, *27*(4), 2012, 2271–2279.

[6] Q. Morante, N. Ranaldo, A. Vaccaro, and E. Zimeo, Pervasive grid for large-scale power systems contingency analysis, *IEEE Transactions on Industrial Informatics*, *2*(3), 2006, 165–175.

[7] Z. Ma, S. Wang, S. Li, and Y. Shi, Long-term coordination for hydro-thermal-wind-solar hybrid energy system of provincial power grid, *Energy Procedia*, *158*, 2019, 6231–6235.

[8] M. Saeedi, M. Moradi, M. Hosseini, A. Emamifar, and N. Ghadimi, Robust optimization based optimal chiller loading under cooling demand uncertainty, *Applied Thermal Engineering*, *148*, 2019, 1081–1091.

[9] W. Gao, A. Darvishan, M. Toghani, M. Mohammadi, O. Abedinia, and N. Ghadimi, Different states of multi-block based forecast engine for price and load prediction, *International Journal of Electrical Power & Energy Systems*, *104*, 2019, 423–435.

[10] N. Kumar, I. Hussain, B. Singh, and B.K. Panigrahi, MPPT in dynamic condition of partially shaded PV system by using wode technique, *IEEE Transactions on Sustainable Energy*, *8*(3), 2017, 1204–1214.

[11] M.I. Alomoush, Application of the stochastic fractal search algorithm and compromise programming to combined heat and power economic–emission dispatch, *Engineering Optimization*, 2019, 1–19.

[12] K. Zervoudakis and S. Tsafarakis, A Mayfly optimization algorithm, *Computers & Industrial Engineering*, 2020, 106559.

[13] R. Eberhart and J. Kennedy, Particle swarm optimization, *Proceedings of the IEEE International Conference on Neural Networks*, vol. 4. Citeseer, 1995, 1942–1948.

[14] R.B. Goldberg, S.J. Barker, and L. Perez-Grau, Regulation of gene expression during plant embryogenesis, *Cell*, *56*(2), 1989, 149–160.

[15] J. Wright, A.Y. Yang, A. Ganesh, S.S. Sastry, and Y. Ma, Robust face recognition via sparse representation, *IEEE Transactions on Pattern Analysis and Machine Intelligence*, *31*(2), 2008, 210–227.

[16] M. Cornick, B. Hunt, E. Ott, H. Kurtuldu, and M.F. Schatz, State and parameter estimation of spatiotemporally chaotic systems illustrated by an application to Rayleigh–Bénard convection, *Chaos: An Interdisciplinary Journal of Nonlinear Science*, *19*(1), 2009, 013108.

[17] K. Shahna and A. Mohamed, A novel image encryption scheme using both pixel level and bit level permutation with chaotic map, *Applied Soft Computing*, *90*, 2020, 106162.

[18] S.A. Gaganpreet Kaur, Chaotic whale optimization algorithm, *Journal of Computational Design and Engineering*, *5*, 2018, 275–284.

[19] K. Dasgupta, P.K. Roy, and V. Mukherjee, Power flow based hydro-thermal-wind scheduling of hybrid power system using sine cosine algorithm, *Electric Power Systems Research*, *178*, 2020, 106018.

[20] O. Abedinia, M. Zareinejad, M.H. Doranehgard, G. Fathi, and N. Ghadimi, Optimal offering and bidding strategies of renewable energy based large consumer using a novel hybrid robust-stochastic approach, *Journal of Cleaner Production*, *215*, 2019, 878–889.

[21] N. Ghadimi, A. Akbarimajd, H. Shayeghi, and O. Abedinia, Two stage forecast engine with feature selection technique and improved meta-heuristic algorithm for electricity load forecasting, *Energy*, *161*, 2018, 130–142.

Biographies

Kingsuk Majumdar received his M. Tech in Electrical Engineering from NIT, Durgapur, 2013. He is an assistant Professor in the Department of Electrical Engineering, Dr. B C Roy Engineering College, Durgapur. His research interests include optimization, power system, power electronics, *etc.* He has guided several B. Tech and three M. Tech students. He is an associate member of The Institution of Engineers (India).

Provas K. Roy obtained Ph.D. degree in Electrical Engineering from National Institute of Technology Durgapur in 2011. He received his Master degree in Electrical Machine in 2001 from Jadavpur University. He finished his Engineering studies in Electrical Engineering from Regional Engineering College (presently known as National Institute of Technology), Durgapur. Presently, he is working as a Professor in Electrical Engineering Department at Kalyani Government Engineering College, West Bengal, India. He was the recipient of the Outstanding Reviewer Award for IJEPES (Elsevier, 2018), EAAI (Elsevier, 2017), Renewable Energy Focus (Elsevier, 2018), ASEJ (Elsevier, 2017). He has published more than 150 research papers in National/International Journals and conference and more than 75 Journals published in reputed SCI and Scopus indexed Journals and more than 10 book chapters and two books of international standard. Six research scholars have obtained their Ph.D. degree under his guidance and eight students are perusing their Ph.D. under his guidance. His research interest includes economic load dispatch, optimal power flow, FACTS, automatic generation control, radial distribution network, power system stabilizer, image processing, machine learning, evolutionary techniques, *etc.*

Subrata Banerjee received the Ph.D. degree in electrical engineering from IIT Kharagpur, Kharagpur, India, in 2005. He is currently a Professor with the Department of Electrical Engineering, National Institute of Technology, Durgapur, India. He has successfully completed several research and consultancy projects, including one major from DST, Government of India. He has authored/coauthored about 180 research papers in national/international journals and conference records. He has filed three Indian patents and received one Indian Patent. He has guided nine Ph.D. and 21 M.Tech. students and many are pursuing their degree under his guidance. His research interests include power electronics converters, and application of control systems in power electronics and power systems. He is a Fellow of the Institution of Engineers, India, the Institution of Electronics and Telecommunication Engineers, India, and the Institution of Engineering and Technology, U.K. He was a recipient of several academic awards, including nine Best Paper Awards and the TATA RAO Prize. His biography is included in Marquis Who's Who 2007 and IBC Foremost Engineers of the World 2008. He is acting as an Associate Editor/Editorial Board in IEEE ACCESS, USA, and IET Power Electronics, U.K.